information on dangerous weather conditions. Also, the simulation analysis, especially for areas with high FW density, can be helpful as well as a common sense when deciding on the subsequent connections of the FWs in such areas.

1. Raport grupy zadaniowej UCTE. Energetyka wiatrowa w połączonym systemie elektroenergetycznym // Elektroenergetyka. – 2004. – Nr 4. – S. 17–39. 2. Instrukcji Ruchu i Eksploatacji Sieci Przesyłowej z dn. – 17 marca 2006 r. "Warunki korzystania, prowadzenia ruchu, eksploatacji i planowania rozwoju sieci" – w szczególności rozdział II.B.3.3.3. "Wymagania techniczne i warunki pracy farm wiatrowych" (obowiązuje od 01.06.2006 r.). 3. Grządzielski I., Welenc R., Pluciński T. Algorytmy sterowania farmą wiatrową w normalnych i zakłóceniowych stanach pracy systemu elektroenergetycznego // Energetyka. – 2007. – Nr 1. – S. 9–15. 4. Lubośny Z. Wind Turbine Operation in Electric Power Systems. – Springer-Verlag Berlin Heidelberg, 2003. 5. Sobczak B., Dąbrowski D., Kąkol A., Mazur M. Modelowanie i agregacja generacji wiatrowej w badaniach dynamicznych systemu elektroenergetycznego // Energetyka APE'04. – Czerwiec 2004. – S. 178–185. 6. Claudia M. Murdoch. PSLF/PLOT Manuals. GE PSLF. Modified. – 20 January 2005. 7. Nicholas W. Miller, William W. Price, Juan J. Sanchez – Gasca. Stability Modeling of Vestas V80 Wind Turbine – Generator. GE PSLF, March 2003.

УДК 621.311

J. Büllow[1], I. Doležel[2], P. Karban[1], B. Ulrych[1]
[1]Faculty of Electrical Engineering, UWB, Plzeň, Czech Republic
[2]Faculty of Electrical Engineering, CTU, Czech Republic

NUMERICAL ANALYSIS OF AN MHD MINIPUMP WITH PERMANENT MAGNNETS TRANSPORTING MOLTEN METAL

Розглянуто перекачування невеликих кількостей розплавлених металів, яке ґрунтується на магнітогідродинамічному ефекті, де магнітне поле створюється системою відповідно сконструйованих постійних магнітів. Особливу увагу приділено конструкції пристрою, яка визначається залежно від його геометрії і характеристик. Теоретичні дослідження ілюструються прикладом, результати якого коментуються.

The paper deals with pumping of small amounts of molten metals based on the magnetohydrodynamic effect, where the magnetic field is generated by a system of appropriately arranged permanent magnets. Investigated is particularly the pumping lead of the device as a function of its geometry and field quantities. The theoretical analysis is illustrated on an example whose results are discussed.

Introduction. The magnetohydrodynamic (MHD) effect is a well-known physical phenomenon used in a lot of devices for transporting electrically conductive liquids (see, for example, [1–3]). The effect is based on the interaction of mutually independent time invariable current and magnetic fields that results in a force perpendicular to both of them. In most of these devices the current field in the liquid is generated by a voltage or current source, while the magnetic field is produced by a system of coils (for example of the saddle shape).

The paper deals with a minipump for transporting molten aluminum (Al), where the magnetic field is excited by a system of appropriately arranged permanent magnets. The principal advantage of such a device consists in its technological and operational simplicity; on the other hand the amount of the transported liquid is affected by the parameters of available permanent magnets and cannot be expected to be (on usual conditions) too high.

The analysis starts from the description of the technical problem and building of its mathematical model that is formulated as a weakly coupled electromagnetically-thermo-hydrodynamic task. This model is then solved by appropriate (mostly FEM-based) professional codes supplemented by a number of own scripts and procedures. The methodology is illustrated on an example demonstrating the possibilities of the investigated MHD system.

Formulation of the technical problem. The principle of using of the MHD effect for pumping electrically conductive liquids (among others molten metals) is obvious from Fig. 1a and 1b. The liquid medium **1** flows in channel **2** between two nonferromagnetic (and in case of molten metals also heat-proof) electrodes **E1** and **E2** that deliver direct current I_e whose density $\boldsymbol{J}_e$ is a vector parallel to axis x, perpendicularly to the axis of the channel. A system of permanent magnets **M1**–**M8** (see Fig. 2, see [4]) produces in medium **1** stationary magnetic field whose vector $\boldsymbol{B}_m$ is oriented in direction y, perpendicular both to the axis of the channel and vector $\boldsymbol{J}_e$. The field produced by the magnets **M1**–**M8** must be as strong and uniform as possible. If the working medium is molten metal, it is also necessary to thermally insulate the permanent magnets in order to keep their temperature T_{work} at the prescribed operation level. It must hold that $T_{work} \le T_{max}$ where T_{max} is the maximum acceptable working temperature of the magnets.

The interaction of the above current and magnetic fields gives rise to the volume Lorentz forces in melt. Their integral value (vector $\boldsymbol{F}_L$) is oriented in direction z and pushes the conductive medium upwards.

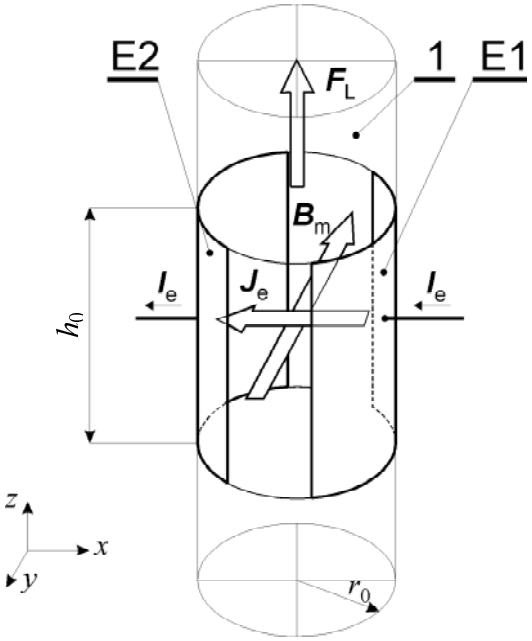

Fig. 1a. The principle of the considered MHD pump. **E1, E2**: *Fire-proof nonferromagnetic electrodes producing the current field* $\boldsymbol{J}_e$ *(the system of permanent magnets producing the magnetic field* $\boldsymbol{B}_m$ *is depicted in Fig. 1b*

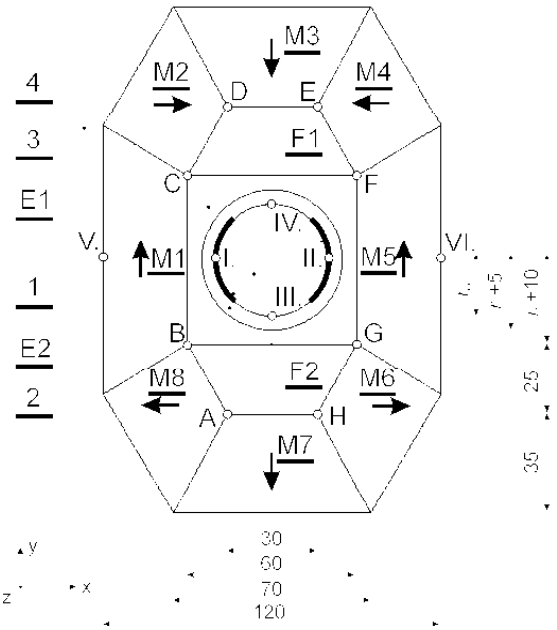

Fig. 1b. The cross-section of the MHD pump (arrangement 1*)* **1 –** *electrically conductive medium,* **2 –** *channel,* **3 –** *thermal insulation,* **4 –** *ambient air,* **E1**, **E2** *– heat-proof electrodes,* **M1**–**M8 –** *permanent magnets,* **F1**, **F2** *– ferromagnetic focusators of magnetic flux*

The paper contains an analysis of five different versions of the working space of the MHD minipump (see Figs. 1b and 2). Its aim is to evaluate them from the viewpoint of its pumping lead h and obtain a sufficient amount of data for a suitable design of the device.

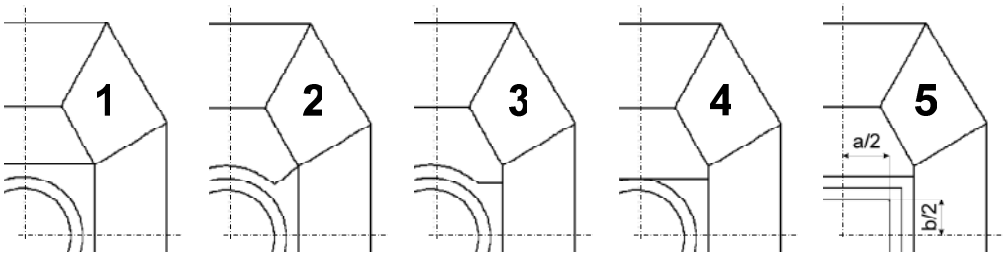

Fig. 2. Arrangements of the investigated channels

Mathematical model and its solution. The full mathematical model of the MHD minipump (with the cross-section corresponding to Fig. 2) describes the

- *stationary electric and current fields* in an electrically conductive and nonferromagnetic liquid medium **1** in channel **2** produced by the current I_{e} flowing from a current source to electrodes **E1** and **E2**,
- *stationary magnetic field* of density $\boldsymbol{B}_{\mathrm{m}}$ in the whole working space of the pump produced by the system of the permanent magnets **M1**–**M8,**
- *stationary temperature field* in the whole working space produced by the liquid medium **1** (molten metal) of temperature T_{work}.

Provided that the cross-section of the channel **2** is much smaller than its length, the problem can be considered 2D and formulated in the system of Cartesian coordinates x, y, z.

The definition area. The definition area of all three fields is obvious from Figs. 1b and 2. In case of the magnetic field it may be (from the physical viewpoint) considered unbounded, but with respect to the consequent numerical solution it has to be bounded by an artificial boundary Γ_{∞} (see further paragraphs) placed at a sufficient distance from the system of magnets **M1**–**M8**.

The differential equations. The stationary electric field may be described (see [5, 6]) by the electric potential φ satisfying the Laplace equation

$$\Delta\varphi = 0 \tag{1}$$

In the area of the channel **2** filled by an electrically conductive liquid this electric field produces the current field given as

$$\boldsymbol{J}_{\mathrm{e}} = -\gamma_{\mathrm{e}} \cdot \operatorname{grad}\varphi \tag{2}$$

where γ_{e} is the electrical conductivity of the liquid medium and $\boldsymbol{J}_{\mathrm{e}}$ the vector of the current density that has generally two components: $\boldsymbol{J}_{\mathrm{e}} = \mathbf{i} \cdot J_x(x, y) + \mathbf{j} \cdot J_y(x, y)$.

The stationary magnetic field may be described in terms of the magnetic vector potential $\boldsymbol{A}$ (see [4, 5]) with only one nonzero component ($\boldsymbol{A} = \mathbf{i} \cdot 0 + \mathbf{j} \cdot 0 + \mathbf{k} \cdot A_{\mathrm{z}}(x, y)$). This potential satisfies general equation

$$\operatorname{curl}\left(\frac{1}{\mu} \operatorname{curl} \boldsymbol{A} - \boldsymbol{H}_{\mathrm{c}} \right) = \mathbf{0}, \tag{3}$$

where $\boldsymbol{H}_{\mathrm{c}}$ denotes the coercive force and occurs only in the region of the magnets and μ is the permeability that corresponds to the particular subregions in the solved domain. The magnetic flux density in the whole area is then given as $\boldsymbol{B} = \operatorname{curl} \boldsymbol{A}$ and has two nonzero components: $\boldsymbol{B}_{\mathrm{m}} = \mathbf{i} \cdot B_x(x, y) + \mathbf{j} \cdot B_y(x, y)$.

The resultant Lorentz force $\boldsymbol{F}_{\mathrm{L}} = \mathbf{i} \cdot 0 + \mathbf{j} \cdot 0 + \mathbf{k} \cdot F_{\mathrm{L},z}$ acting on the liquid medium in the working space **1** of volume $V_0 = S_0 h_0$ in channel **2** can be determined from integral

$$\boldsymbol{F}_{\mathrm{L}} = \int_{V_0} \left(\boldsymbol{J}_{\mathrm{e}} \times \boldsymbol{B}_{\mathrm{m}} \right) \cdot \mathrm{d}V \tag{4}$$

where S_0 is the area of the channel cross-section, h_0 its active length and the pumping lead h_p is given by relation

$$h_\mathrm{p} = \frac{F_{\mathrm{L},z}}{\rho_\mathrm{e} g S_0} \tag{5}$$

where ρ_e is the specific mass of melt.

The stationary temperature field in the system can be described by equation [7]

$$\mathrm{div}\left(\lambda_\mathrm{T} \cdot \mathrm{grad}\, T\right) = 0 \tag{6}$$

where λ_T the thermal conductivity. The Joule losses in melt are very low and can be neglected without any significant error.

The boundary conditions. The boundary conditions for the electric and magnetic field are exclusively of the first and second kind and are obvious from the physical context of the problem. In case of the temperature field the condition of the first kind occurs along the interface between the transported medium **1** (molten metal of the temperature T_work) and internal wall of the channel **2** or electrodes **E1** and **E2** (see Fig. 2), while the external walls of the system of permanent magnets **M1**–**M8** are characterized by the condition of the heat convection between the system and surrounding air.

The computer model and accuracy of the results. The presented model was solved by the FEM-based code QuickField 5 [8] supplemented with a number of procedures and scripts developed and written by the authors. Particular attention was paid to both position of the fictitious artificial boundary Γ_∞ and numerical convergence of the results. The discretization mesh satisfying the demands on accuracy of three valid digits contained 120000 – 150000 nodes, in the dependence of the arrangement solved (see Fig. 2).

An illustration of possibilities of the numerical solution is presented in Fig. 3 containing the distribution of the calculated equipotential lines and vectors $\boldsymbol{J}_\mathrm{e}$ of the current field for the arrangement No. 2 (Fig. 2) and Fig. 4 showing the calculated distribution of the magnetic force lines in the same arrangement. It is obvious that such maps of both fields provide a sufficient amount of information about suitability of particular arrangements of the MHD pumps: the more uniform are the fields and denser both systems of isolines, the greater will be the Lorentz force $\boldsymbol{F}_\mathrm{L}$ and pumping lead h_p of the device.

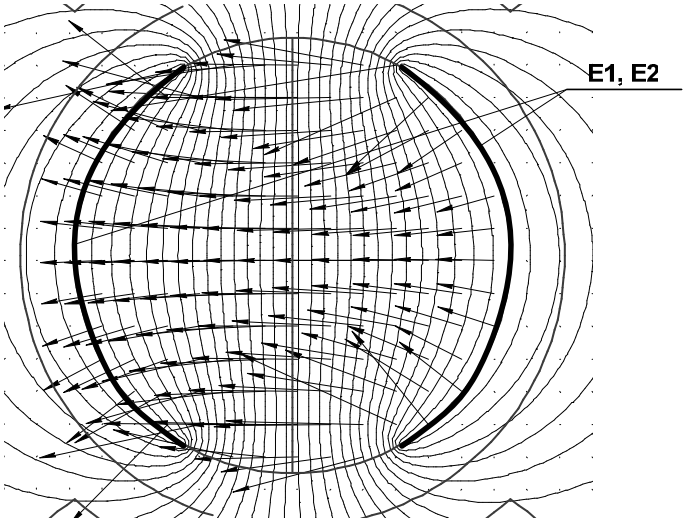

Fig. 3. The calculated distribution of the equipotential lines and vectors $\boldsymbol{J}_\mathrm{e}$ *of the current field in the cross-section of the pump for the arrangement No. 2, in Fig. 2,* $r_0 = 0.02$ *m*

Analogously, Fig. 5 shows the distribution of the steady-state temperature field for the arrangements 2 (Fig. 2) of the pump. It is obvious that this arrangement 2 satisfies a sufficient reduction of the temperature inside relatively uniform thermal insulation **3**.

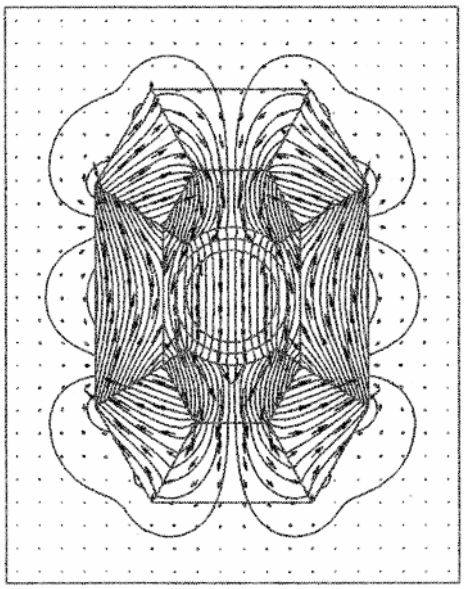

Fig. 4. The calculated distribution of the magnetic f orce lines in the cross-section of the pump for the arrangement No. 2

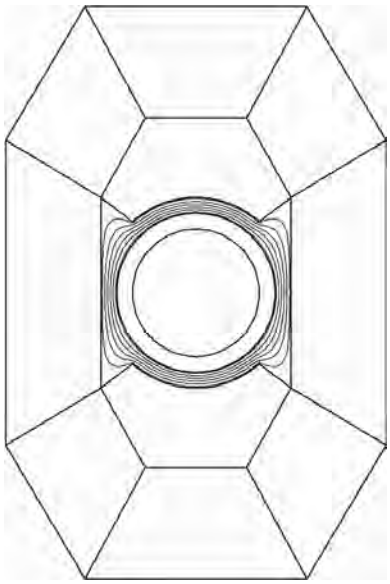

Fig. 5. Distribution of the stationary temperature field – arrangement No. 2 (the step between the individual isotherms $\Delta T = 100$ *°C)*

Illustrative example. The aim of the presented example is to evaluate the considered arrangements of the MHD pump (see Fig. 2) from the viewpoint of the pumping lead h_{p} and to analyze various aspects that may exhibit some influence on this quantity.

Technical data and discussion of the results. The arrangements and basic dimensions of all versions of the MHD pump are obvious from Figs. 1a, 1b and 2.

The cross-section of the working channel **2** is

- for arrangements 1–4: $S_0 = \pi r_0^2$, for basic radius $r_0 = 0.02$ m $S_0 = 1.257 \cdot 10^{-3}\,\mathrm{m}^2$,
- for arrangement 5: $S_0 = ab$, for $a = 0.04$ m and $b = 0.0314$ $S_0 = 1.257 \cdot 10^{-3}\,\mathrm{m}^2$.

Equality of both cross-sections allows an objective comparison of both arrangements. The working length of the pump (length of the working channel **2** filled in by the transported medium **1** affected by both electric and magnetic field and consequent Lorentz force $\boldsymbol{F}_{\mathrm{L}}$, see Fig. 1a) $h_0 = 0.1\mathrm{m}$ and this quantity corresponds to the value V_0 in integral (4).

The physical parameters of materials used for the construction of the MHD pump are listed in Tab. 1. The table, however, also contains quantities that cannot be described by a single value, such as the temperature dependencies of the electrical and thermal conductivities or the magnetization characteristic of the permanent magnets **M1**–**M8** and focusators **F1**, **F2**. These dependencies (in Tab. 1 denoted as **char**.) were taken over from the given references.

The most important quantitative results are listed in Tabs. 2 and 3. From the viewpoint of the pumping lead h_{p} the most advantageous is the version 5 with the rectangular channel or the version 2 with the circular channel (see Fig. 2). But version 5 is somewhat worse from the viewpoint of the temperature rise of the permanent magnets. Even when their average temperature is higher by only 16° C (compared with the version 2) there may appear worse conditions of flow connected with higher hydrodynamic friction in the rectangular channel.

Table 1

The physical parameters of materials used in the pump

element	Material	parameter	value	unit
working medium	molten Al [9], [10], [11]	melting temperature T_m	660.32	°C
1		working temperature T_{work}	700	°C
		specific mass ρ_m	$2.375 \cdot 10^3$	kg/m^3
		electrical conductivity γ_e	$9.709 \cdot 10^6$	S/m
		thermal conductivity* λ_T	229	W/mK
working channel	a**) EUCOR [12]	thermal conductivity λ_T	**char.**	
2		max. working temp. T_{max}	1000	°C
	b***) ZrO_2 [13]	thermal conductivity λ_T	2	W/mK
		electrical conductivity γ_e	$<10^{-12}$	S/m
		max. working temp. T_{max}	1500	°C
thermal insulation	glass wool [9]	thermal conductivity λ_T	0.03–0.05	W/mK
3				
permanent magnets	N_27SH [14]	coercive force H_c	780	kA/m
M1–**M8**		remanence B_r	1.11	T
		permeability μ_r	1.132	-
		thermal conductivity λ_T	8.972	W/mK
		electrical conductivity γ_e	69.44	S/m
		max. working temp. T_{max}	150	°C
electrodes	austenitic heat-proof steel	permeability μ_r	1	-
E1, **E2**	[15], ČSN 17 241	electrical conductivity γ_e	$1.5 \cdot 10^6$	S/m
		thermal conductivity λ_T	**char.**	W/mK
		max. working temp. T_{max}	1100	°C
focusators of mag-	carbon steel	characteristic	**char.**	
netic flux **F1**, **F2**	[15], ČSN 12 040	thermal conductivity λ_T	**char.**	W/mK

* At the working temperature $T_{work} = 700$ °C.

** Circular channel, arrangements 1–4.

*** Rectangular channel, arrangement 5.

Table 2

Final results – the influence of the shape of the channel cross-section (see Fig. 2)

arrangement of the pump	$B_{y,avg}$	$J_{x,avg}$	$T_{m,avg}$	$F_{L,z}$	h_p
	(T)	(A/m^2)	(°C)	(N)	(m)
1. (*)	0.61705	-	89	-	-
2. (*)	**0.62633**	$2.632 \cdot 10^5$	100	20.72	0.710
3. (*)	0.59054	-	101	-	-
4. (*)	0.64516	-	331	-	-
5. (**)	**0.63818**	$3.183 \cdot 10^5$	116	25.51	0.872

(*) circular cross-section of the working channel.

(**) rectangular cross-section of the working channel

both cross-sections are equal.

Table 3

The final results – the influence of radius r_0 of the circular channel

r_0	$B_{y,\mathrm{avg}}$	$J_{x,\mathrm{avg}}$	$F_{\mathrm{L},z}$	h_{p}
(m)	(T)	(A/m^2)	(N)	(m)
0.01	0.78067	$5.265\cdot10^5$	12.91	1.764
0.015	0.69128	$3.509\cdot10^5$	17.15	1.041
0.2	0.62633	$2.632\cdot10^5$	20.72	0.71

Conclusion. The paper shows that the investigated MHD minipumps for transporting electrically conductive, nonferromagnetic liquid medium (molten metals, various conductive liquids such as electrolytes) represent relatively prospective and technically quite real devices. The presented methodology of their numerical modeling allows their optimization from the viewpoint of both the pumping lead and technological aspects (the shape of the working channel, electrodes etc.). It is also necessary to remind that the pumping lead could substantially be increased by connection of several pumps of this kind into series (from the hydraulic viewpoint) with one working channel.

The design of the device requires a considerable attention concerning the thermal insulation of the permanent magnets, whose working temperature limits the final arrangement of the minipump.

Next work in the field will be aimed at the experimental validation of the conclusions following from the presented computational results.

Acknowledgment. *The financial support of the Grant Agency of the Czech Republic (project GA ČR 102/07/0496) and Ministry of Education (Research Plan MSM 6840770017) is gratefully acknowledged.*

1. Kikuchi S., Murakami K. Behavior of a New DC Electromagnetic Pump Using Superconducting Magnet // IEEE Trans. – 1977. – Mag. 13, No. 5. – P. 1559–1561. 2. Takorabet N. Computation of Force Density Inside the Channel of an Electromagnetic Pump by Hermite Projection // IEEE Trans. – 2006. – Mag. 42, No. 3. – P. 430–433. 3. Ma N., Moon T.J., Walker J.S. Electromagnetic Pump with Thin Metal Walls // J. Fluid Engrg., Trans. ASME 116. – 1994. – No. 2. – P. 298–302. 4. Blazkova M. Magnetic Cooling (in Czech) // Pokroky matematiky, fyziky a astronomie. – 2005. – Vol. 50, No. 4. – P. 301–320. 5. Haňka L. Theory of Electromagnetic Field (in Czech) // SNTL/ALFA. – Praha, 1975. 6. Stratton J.A. Electromagnetic Theory. – McGraw-Hill Book Co., NY, 1941. 7. Holman J.P. Heat Transfer. – McGraw-Hill Book Co., NY, 2002. 8. www.quickfield.com. 9. J. Mikulčák et al., Mathematical, Physical and Chemical Tables (in Czech). SPN. – Praha, 1970. 10. http:/en.wikipedia.org/wiki/Aluminum. 11. http:/www.aldebaran.cz/elmg/kurz_06_prou.pdf. 12. www.eutit.cz. 13. http://www.accuratus.com/ index.htm. 14. www.macmillmagnet.com. 15. Factory Standard SKODA SN 006004 (in Czech).